

A Magnetohydrodynamic Model for the Formation of Episodic Jets

Feng Yuan^{1,2}, Jun Lin^{3,4}, Kinwah Wu⁵, and Luis C. Ho⁶

ABSTRACT

Episodic ejection of plasma blobs have been observed in many black hole systems. While steady, continuous jets are believed to be associated with large-scale open magnetic fields, what causes the episodic ejection of blobs remains unclear. Here by analogy with the coronal mass ejection on the Sun, we propose a magnetohydrodynamical model for episodic ejections from black holes associated with the closed magnetic fields in an accretion flow. Shears and turbulences of the accretion flow deform the field and result in the formation of a flux rope in the disk corona. Energy and helicity are accumulated and stored until a threshold is reached. The system then loses its equilibrium and the flux rope is thrust outward by the magnetic compression force in a catastrophic way.

Subject headings: accretion, accretion disks — black hole physics — galaxies: active — galaxies: jets — quasars: general

1. Introduction

Jets are ubiquitous in astrophysical accreting systems. Large-scale jets tend to be steady and continuous. There are also intermittent, episodic outflows from the accretion systems,

¹Shanghai Astronomical Observatory, Chinese Academy of Sciences, 80 Nandan Road, Shanghai 200030, China; fyuan@shao.ac.cn

²Joint Institute for Galaxy and Cosmology (JOINGC) of SHAO and USTC

³National Astronomical Observatories/Yunnan Observatory, Chinese Academy of Sciences, Kunming 650011, China; jlin@ynao.ac.cn

⁴Harvard-Smithsonian Center for Astrophysics, 60 Garden Street, Cambridge, MA 02138, USA

⁵Mullard Space Science Laboratory, University College London, Holmbury St Mary, Surrey RH5 6NT, UK; kw@mssl.ucl.ac.uk

⁶The Observatories of the Carnegie Institution of Washington, 813 Santa Barbara Street, Pasadena, CA 91101, USA; lho@ociw.edu

which are associated with flare emission. In Sgr A*, the massive black hole in the Galactic center, radio, infrared and X-ray flares occur several times a day (Eckart et al. 2006), showing delays among the peaks in the light curves at different wavebands (Yusef-Zadeh et al. 2006). The delays, together with the fast rise and slow decay in the brightness and the polarization of the flare emission, are attributed to the ejection and expansion of plasmons from the accretion flow (Yusef-Zadeh et al. 2006; van der Laan 1966). However, despite its close distance, continuous jets have not been detected in Sgr A* even with the highest VLBI resolution. X-ray and radio monitoring observations of the active galaxy 3C 120 over three years also showed episodic ejections, in the form of bright superluminal knots (Marscher et al. 2002). Such knots in jets are very common in active galactic nuclei (e.g., M 87). They are usually explained by the collisions of shells ejected from the central engine. It has been proposed that plasmon ejections should be considered transient or “type II” jets (Fender & Belloni 2004; Fender, Belloni & Gallo 2004).

Similar plasmon ejections have also been observed in Galactic microquasars, such as GRS 1915+105 (Mirabel & Rodriguez 1994; Mirabel et al. 1998; Fender et al. 1999), GRO J1655–40 (Hjellming & Rupen 1995), and XTE J1550–564 (Corbel et al. 2002). Brief, intense radio flares, accompanied by X-ray flares (and infrared flares as well in GRS 1915+105) are observed during the transition from the hard X-ray spectral state to the soft X-ray spectral state. The flares have been associated with the ejections of plasmons, as in the case of Sgr A*. The presence of plasmon ejections in Sgr A* is based on interpretation of the simultaneous light curves at different wavebands. By contrast, plasmon ejecta from microquasars are often clearly resolvable in radio images, and they convincingly show relativistic motion away from the central core.

The characteristics of episodic plasmon ejections and steady, continuous jets are distinguishable. Both kinds of outflows have been observed in the same individual microquasar. While episodic ejections occur during the transition from the hard to the soft state (Fender, Belloni & Gallo 2004), continuous jets are seen only in the hard state. Observations generally show larger Lorentz factor for transient jets (Fender, Belloni & Gallo 2004). Also, their radio spectrum evolves rapidly and the emission becomes optically thin, in contrast to continuous jets whose bright radio emission remains opaque. There is evidence that the emission from ejected plasmons is more highly polarized than the emission from the continuous jets (Fender & Belloni 2004).

Magnetohydrodynamical numerical simulations of accretion flows assuming a weak initial magnetic field have shown impulsive mass ejections embedded in steady, continuous jet-like outflow (Machida, Hayashi & Matsumoto 2003; De Villiers, Hawley & Krolik 2003). The ejection events are quasi-periodic, and the time interval between successive ejections is

roughly $1600 \text{ GM}/c^3$ (De Villiers, Hawley & Krolik 2003), where G , c and M are the gravity constant, the speed of light, and the black hole mass, respectively. For parameters appropriate for Sgr A*, the time interval is ~ 6 hours. If we assume that each flare of reasonably high intensity is associated with an ejection event, this timescale is consistent with those seen in current observations (Yusef-Zadeh et al. 2006).

The formation of the continuous jets has been widely studied and models have been proposed (e.g., Blandford & Znajek 1977; Blandford & Payne 1982). However, the origin of episodic jets has remained unclear. In this paper, by analogy with the coronal mass ejection (CME) phenomena in the Sun, we propose a magnetohydrodynamical model for episodic jets (§2). We then explain how to understand the above-mentioned various observations characteristic of episodic jets based on this model (§3). Specifically, our calculations show that for parameters appropriate for the black hole in our Galactic center, the plasmon can attain relativistic speeds in about 35 minutes.

2. An MHD model for episodic jets

We note that two-component magnetic outflows/ejections have been found in a variety of astrophysical environments. A well-studied system is the outflows of the Sun consisting of solar winds and coronal mass ejections (CMEs). The solar wind is relatively steady, continuous and smooth. It originates from the solar surface regions with open magnetic field lines. CMEs are, however, episodic, and they are ejected from coronal regions with closed magnetic field lines (magnetic arcades). The speeds of CMEs can reach up to 2000 km s^{-1} and beyond. The rate of CME occurrence varies from once a few weeks during the solar minimum to several times per day at solar maximum (Zhang & Low 2005; Lin, Soon & Baliunas 2003).

In the Sun, magnetic arcades generally emerge into the tenuous corona from the denser solar photosphere, with their footpoints anchored in the photosphere. The configuration of the coronal magnetic field is thought to be controlled by convective turbulences in the solar photosphere because of the freezing of the field to the plasma. Convective turbulence motion in the photospheric plasma leads to the formation of coronal flux ropes, manifested as dark filaments and bright prominences in observations (Zhang & Low 2005). The ropes are in an equilibrium configuration when there is a balance between the forces due to magnetic compression and magnetic tension from below and above the flux rope (refer to Figure 1a). Nevertheless, the equilibrium is temporary. The turbulences in the photosphere inevitably cause a build-up of stress and helicity. They also convert the kinetic energy in the photosphere into the magnetic energy in the corona (Zhang & Low 2005; Lin, Soon & Baliunas

2003). When the energy accumulation exceeds a certain threshold, the confinement in the magnetic arcade breaks down, and the flux rope gets thrust outward in a catastrophic manner (Forbes & Isenberg 1991; Lin & Forbes 2000; Lin, Soon & Baliunas 2003)¹ Then the magnetic field is severely stretched and a neutral region — the current sheet — develops, separating magnetic fields of opposite polarity (refer to Figure 1b). Dissipation, facilitated by microscopic plasma instabilities, leads to rapid magnetic reconnection in the current sheet (Lin & Forbes 2000; Lin, Soon & Baliunas 2003). This then greatly relaxes the magnetic tension and helps the compression push the rope through the corona smoothly, developing into a CME. On the one hand, magnetic reconnection converts the stored magnetic energy into the microscopic particle kinetic energy in the plasma, which ignites the radiative flares; on the other hand, it transfers the magnetic energy into bulk kinetic energy that propels CME propagation (Zhang & Low 2005; Lin & Forbes 2000). The timescale of the above process of magnetic energy release is determined by the local Alfvén one.

Interestingly, the rate of intermittent ejections from Sgr A* (Yusef-Zadeh 2006) is not far different from the rates of solar CMEs. The similar morphology and characteristics between the outflow components in accreting black holes and in the Sun indicates the operation of a common physical mechanism. We therefore seek to build a model for the magnetic outflows in accreting black holes in light of current understanding of magnetic outflows in the solar environment. In current models for continuous jets, a large-scale open magnetic field is required to extract energy from the rotation of the black hole or the flow in the accretion disk (Blandford & Znajek 1977; Blandford & Payne 1982). If continuous jets correspond to the smooth solar wind component, we propose that the transient, type-II jets are analogous to CMEs, which result from the disruption of closed field lines in the corona above the accretion disk.

In addition to observational evidence mentioned above, there are compelling theoretical reasons to believe similar physical processes operate in accreting black hole and in the solar environment. Numerical simulations have shown that the structure of a hot accretion flow — a cool, dense disk enveloped by a hot corona (Machida, Hayashi & Matsumoto 2000; De Villiers, Hawley & Krolik 2003; De Villiers et al. 2005) — is very similar to the solar atmosphere. An accretion disk with angular momentum transport regulated by magneto-rotational instability is intrinsically turbulent (Balbus & Hawley 1998). Loops of magnetic field emerge into the disk corona. Since their foot points are anchored in the accretion flow which is differentially rotating and turbulent, reconnections and flares occur subsequently

¹ How to determine the timescale of the above energy accumulation process is still an open question. It should be related to the energy transfer speed from the photosphere to the corona, which is determined by the Alfvén timescale, and the value of the threshold energy.

(Blandford 2002; Hirose et al. 2004; Machida, Nakamura, & Matsumoto 2004). We believe that this mechanism gives rise to the flares in Sgr A* that are not accompanied by a CME-type event.

We argue that the above scenario can develop into a more catastrophic situation. The reconnection process changes the magnetic field topology (see Figure 1). It also redistributes the helicity and stores most of it in a flux rope floating in the disk corona, resembling what happens in the Sun (Zhang & Low 2005). The magnetic configuration continues to evolve, after the formation of the flux rope. The system eventually loses the equilibrium, rapidly expelling the flux rope, and a long current sheet develops behind the break-away flux rope (see Forbes & Isenberg 1991; Lin & Forbes 2000 and Figure 1b). Magnetic reconnection then occurs in the sheet, propelling the flux rope away from the accretion disk, giving rise to the accretion disk CME. This process can occur at any radius, but should be much stronger in the innermost region where the magnetic field is much stronger and the emergence of magnetic loops is much more frequent. The process also causes intensive heating in the accretion disk and its corona (Lin, Soon & Baliunas 2003; Lin & Forbes 2000). The radiations from the impulsively heated plasma in the accretion disk and corona will appear as flares in the observations. Such a scenario implies that flares are not purely radiative but also dynamical, and provides a very natural explanation to the flares that are often associated with mass ejection events, as observed in microquasars and Sgr A*.

3. Interpreting various observations characteristic of episodic jets

We now elaborate how plasmons (flux ropes) from the accretion disk corona evolve and propagate in the framework of the CME catastrophe model (Lin & Forbes 2000). We use Sgr A* as an illustration, as its accretion flow is relatively well understood, providing us with reliable estimates of the density, temperature and magnetic field in the accretion flow (Yuan, Quataert & Narayan 2003). Consider a plasmon confined in a coronal magnetic field. It is subject to gravity and magnetic forces (Lin, Mancuso, & Vourlidas 2006); gas pressure can be neglected since it is assumed to be small compared to the magnetic pressure. The plasmon is in a critical position, where the loss of equilibrium starts occurring and the plasmon will be thrust outward. After the catastrophic loss of equilibrium, the upward motion of the flux rope is governed by:

$$m \frac{d^2 h}{dt^2} = \frac{1}{c} |\mathbf{I} \times \mathbf{B}_{\text{ext}}|_h - F_g , \quad (1)$$

where m is the total mass inside the flux rope per unit length, h is the height of the flux rope from the surface of the accretion disk, F_g is the gravitational force, I is the integration of the electric current intensity \vec{j} inside the flux rope, and B_{ext} is the total magnetic field

from all the sources except I , which includes those inside the disk, on the disk surface, and the current sheet. Both the current and magnetic field within and outside of the flux rope satisfy the following conditions (see Lin & Forbes 2000 for details):

$$\mathbf{j} \times \mathbf{B} = 0, \quad (2)$$

$$\mathbf{j} = \frac{c}{4\pi} \nabla \times \mathbf{B}. \quad (3)$$

We choose (x, y) coordinate with $y = 0$ being the equatorial plane and $x = 0$ being the rotation axis of the accretion flow. Suppose that the flux rope is initially located at $(x, y) = (5r_g, 10r_g)$, where $r_g \equiv GM/c^2 = 5.9 \times 10^{11} \text{cm}$ is the gravitational radius of the black hole in Sgr A*. Based on studies of the accretion flow and its corona in Sgr A* (Yuan, Quataert & Narayan 2003; De Villiers, Hawley & Krolik 2003), we set the density of the rope to $n_0 = 10^5 \text{cm}^{-3}$ and the magnetic field to $B_0 = 16 \text{ G}$. The rate of magnetic reconnection, namely the Alfvén Mach number M_A , is taken as 0.1 here. It is the reconnection inflow speed compared to the local Alfvén speed near the current sheet.

The distribution of the density and magnetic field of the corona along the vertical height are very uncertain. Without losing generality, we boldly assume that they are similar to those in the solar atmosphere, which allows us to directly adopt the well-studied models for the solar environment (Lin, Mancuso, & Vourlidas 2006). This assumption can be justified because the results do not change significantly unless the Alfvén speed decreases very rapidly with height within the region of interest, which is unlikely given the planar configuration of the disk corona. Solving equation (1) yields the velocity evolution of the flux rope as shown by Figure 2 (see Appendix for details). Our calculations show the flux rope can be easily accelerated to a speed of $0.8c$ in about 35 minutes.

We now assess the CME scenario using four observational characteristics of episodic transient jets.

(i) *Hard to soft X-ray spectral state transition in microquasars.* The hard state of microquasars is characterized by a steady hot accretion flow. During the transition from the hard state to the soft state, the accretion flow changes rapidly from a hot phase to a cold phase. The collapse of the accretion flow may lead to a temporal eclipse of the continuous jet (Livio, Ogilvie & Pringle 1999; Fender, Belloni & Gallo 2004). The magnetic field in the cold disk is strongly amplified because of the conservation of the magnetic flux during the collapse process. Such a field configuration is highly unstable, and as a consequence substantial magnetic flux will be expelled out from the disk (Pringle, Rees, & Pacholczyk 1973; Shibata, Tajima & Matsumoto 1990). The readjustment of the field provides the free energy to drive “CME” and power the radiative flares. This naturally explains the

observed ejection of plasmons and the radio and X-ray flares observed in the hard to soft state transition in microquasars (Fender, Belloni & Gallo 2004).

(ii) *Large Lorentz factor.* During the disk collapse, a large amount of magnetic energy is liberated on a shorter timescale. The acceleration of the plasmon ejecta is facilitated by this impulsive energy release, which is in contrast to the smooth injection of energy by an ordinary, steady hot accretion flow that launches the continuous jet. It is not surprising that the ejected plasmons should have a larger Lorentz factor than the continuous jet.

(iii) *Optically thin emission and strong polarization.* Particles are accelerated in the magnetic reconnection current sheet as well as in shocks formed when the high-speed plasmons pass through the interstellar medium. The radio flares are due to synchrotron radiation from the accelerated relativistic electrons; the X-ray flares are probably caused by bremsstrahlung, synchrotron-self-Comptonization, or also synchrotron radiation. Unlike a normal continuous jet, the plasmon ejecta are single blobs. They expand almost adiabatically after leaving the accretion disk and can quickly become optically thin in the radio band. The high degree of polarization is simply a consequence of the presence of a relatively ordered magnetic field enclosing the ejecta and the small optical depth in the substantially inflated plasmon blobs.

(iv) *Presence of bright knots.* The accretion disk corona is threaded by both open and closed magnetic fields, allowing the coexistence of continuous and transient type II jets. The interaction of the very high-speed ejected plasmon blobs with the slow preexisting continuous jet could easily lead to shock formation, which will appear as bright knots embedded in steady continuous jet.

We thank J. E. Pringle, D. Uzdensky, and F. Yusef-Zadeh for comments. This work was supported by the Natural Science Foundation of China (grants 10773024, 10833002, 10821302, 10825314, and 40636031), One-Hundred-Talent Program of CAS, and the National Basic Research Program of China (grants 2009CB824800 and 2006CB806303). J.L. was supported also by the Chinese Academy of Sciences (grant number KJCX2-YW-T04) and NASA (grant number NNX07AL72G) when visiting CfA.

A. Solving Equation (1)

In this section we describe how we solve equation (1). The first term in equation (1) results from the electromagnetic interaction that reads

$$F_m = \frac{B_0^2 \lambda^4}{8hL_{PQ}^2} \left[\frac{H_{PQ}^2}{2h^2} - \frac{(\lambda^2 + p^2)(h^2 - q^2)}{\lambda^2 + h^2} - \frac{(\lambda^2 + q^2)(h^2 - p^2)}{\lambda^2 + h^2} \right], \quad (\text{A1})$$

where $L_{PQ}^2 = (\lambda^2 + p^2)(\lambda^2 + q^2)$, $H_{PQ}^2 = (h^2 - p^2)(h^2 - q^2)$, B_0 and λ are the average field strength and the length scale of the magnetic field source on the disk surface, respectively, h , p , and q are the heights of the flux rope center and the lower and upper tips of the current sheet from the disk surface, respectively (refer to the right panel in Figure 1).

Here the first term in the square brackets at the right hand side of equation (A1) results from the interaction between the body electric current inside the flux rope and the surface current flowing on the disk surface. The resulting force, which is also known as the magnetic compression, pushes the flux rope outwards (upwards). The other two terms in the brackets come from the interaction of the body current inside the rope with those inside the current sheet and the accretion disk (not including the surface current). The resulting force, also known as the magnetic tension, tends to pull the flux rope backwards (downwards). With the loss of equilibrium in the system occurring, the compression dominates the tension. So the flux rope is thrust outward in a catastrophic fashion.

The equations that govern the dynamic behaviors of p and q are given by

$$\frac{dp}{dt} = p'\dot{h}, \quad \frac{dq}{dt} = q'\dot{h}, \quad \frac{d\dot{h}}{dt} = \dot{h}'\dot{h}, \quad \frac{dh}{dt} = \dot{h}, \quad (\text{A2})$$

where \dot{h} is the velocity of the flux rope, $p' = dp/dh$, $q' = dq/dh$, and $d^2h/dt^2 = \dot{h}'\dot{h}$. (Note: Expressing the above ordinary differential equations and the related parameters in their present forms is for convenience of applying an existing code, *Mathematica*, to integrating these equations.)

Furthermore, p' and q' are related to other parameters such that

$$\begin{aligned} p' &= \frac{\tilde{A}_{0h}A_{Rq} - A_{Rh}A_{0q}}{A_{Rp}A_{0q} - A_{0p}A_{Rq}}, \\ q' &= \frac{A_{Rh}A_{0p} - \tilde{A}_{0h}A_{Rp}}{A_{Rp}A_{0q} - A_{0p}A_{Rq}}, \end{aligned} \quad (\text{A3})$$

with

$$\tilde{A}_{0h} = \frac{M_A B_y^2(0, y_0)}{B_0 \lambda \dot{h} \sqrt{4\pi\rho(y_0)}} - A_{0h},$$

where

$$\begin{aligned}
A_{0p} &= \frac{\lambda p(h^2 + \lambda^2)(\lambda^2 + q^2)}{h^2 q [(\lambda^2 + p^2)(\lambda^2 + q^2)]^{3/2}} \left[(h^2 - q^2) \Pi \left(\frac{p^2}{h^2}, \frac{p}{q} \right) - h^2 K \left(\frac{p}{q} \right) \right] \\
A_{0q} &= \frac{\lambda(h^2 + \lambda^2)(\lambda^2 + p^2)}{h^2 [(\lambda^2 + p^2)(\lambda^2 + q^2)]^{3/2}} \left[(h^2 - q^2) \Pi \left(\frac{p^2}{h^2}, \frac{p}{q} \right) - h^2 K \left(\frac{p}{q} \right) \right] \\
A_{0h} &= -\frac{\lambda}{h^3 q \sqrt{(\lambda^2 + p^2)(\lambda^2 + q^2)}} \left[h^2 q^2 E \left(\frac{p}{q} \right) - h^2 (h^2 + q^2) K \left(\frac{p}{q} \right) \right. \\
&\quad \left. + (h^4 - p^2 q^2) \Pi \left(\frac{p^2}{h^2}, \frac{p}{q} \right) \right], \tag{A4}
\end{aligned}$$

and

$$\begin{aligned}
A_{Rp} &= \frac{\lambda p(h^2 + \lambda^2)}{q(\lambda^2 + p^2)^2} \sqrt{\frac{\lambda^2 + p^2}{\lambda^2 + q^2}} \left\langle \left(1 - \frac{p^2}{h^2} \right) \Pi \left[\sin^{-1} \left(\frac{q}{h} \right), \frac{p^2}{h^2}, \frac{p}{q} \right] \right. \\
&\quad \left. - F \left[\sin^{-1} \left(\frac{q}{h} \right), \frac{p}{q} \right] - \frac{q}{2h} \sqrt{\frac{h^2 - q^2}{h^2 - p^2}} \left\{ 1 + \ln \left[\frac{\lambda H_{PQ}^3}{r_{00} L_{PQ} (h^4 - p^2 q^2)} \right] \right\} \right\rangle, \\
A_{Rq} &= \frac{\lambda(h^2 + \lambda^2)}{(\lambda^2 + q^2)^2} \sqrt{\frac{\lambda^2 + q^2}{\lambda^2 + p^2}} \left\langle \left(1 - \frac{p^2}{h^2} \right) \Pi \left[\sin^{-1} \left(\frac{q}{h} \right), \frac{p^2}{h^2}, \frac{p}{q} \right] \right. \\
&\quad \left. - F \left[\sin^{-1} \left(\frac{q}{h} \right), \frac{p}{q} \right] - \frac{q}{2h} \sqrt{\frac{h^2 - p^2}{h^2 - q^2}} \left\{ 1 + \ln \left[\frac{\lambda H_{PQ}^3}{r_{00} L_{PQ} (h^4 - p^2 q^2)} \right] \right\} \right\rangle, \\
A_{Rh} &= \frac{\lambda}{2h^2 L_{PQ} H_{PQ}} \left\{ \frac{2h^6 - 2(\lambda p q)^2}{h^2 + \lambda^2} - \frac{h^2(p^2 + q^2)(h^2 - \lambda^2)}{h^2 + \lambda^2} \right. \\
&\quad \left. + (h^4 - p^2 q^2) \ln \left[\frac{\lambda H_{PQ}^3}{r_{00} L_{PQ} (h^4 - p^2 q^2)} \right] \right\} \\
&\quad + \frac{\lambda}{h q L_{PQ}} \left\{ (h^2 + q^2) F \left[\sin^{-1} \left(\frac{q}{h} \right), \frac{p}{q} \right] - q^2 E \left[\sin^{-1} \left(\frac{q}{h} \right), \frac{p}{q} \right] \right. \\
&\quad \left. - \left(h^2 - \frac{p^2 q^2}{h^2} \right) \Pi \left[\sin^{-1} \left(\frac{q}{h} \right), \frac{p^2}{h^2}, \frac{p}{q} \right] \right\}. \tag{A5}
\end{aligned}$$

Here K , E , and Π in (A4) are first, second, and third kinds of complete elliptic integrals, respectively; F , E , and Π in (A5) are first, second, and third kinds of incomplete elliptic integrals, respectively. Deducing these equations is tedious and time-consuming, we do not duplicate the approach here. Readers are referred to our previous works for detail(15; 16).

The magnetic configuration involved in the formulation above is described by

$$B_y(x, y) + iB_x(x, y) = \frac{iB_0 \lambda^2 (h^2 + \lambda^2) \sqrt{(z^2 + p^2)(z^2 + q^2)}}{(z^2 - \lambda^2)(h^2 + z^2) \sqrt{(\lambda^2 + p^2)(\lambda^2 + q^2)}}, \tag{A6}$$

where B_x and B_y are x and y components of the magnetic field, both of them are functions of x and y , $i = \sqrt{-1}$, and $z = x + iy$. This expression includes contributions from the background field, the currents flowing in the flux rope, in the current sheet, and on the disk surface. More discussions on this issue are available in (16) and references therein.

From (A6), B_y in the expression for \tilde{A}_{0h} thus reads as

$$B_y(0, y) = \frac{B_0 \lambda^2 (h^2 + \lambda^2) \sqrt{(y^2 - p^2)(q^2 - y^2)}}{(y^2 + \lambda^2)(h^2 - y^2) \sqrt{(p^2 + \lambda^2)(q^2 + \lambda^2)}} \quad (\text{A7})$$

for $p \leq y \leq q$. Here $y_0 = (p + q)/2$ is the height of the current sheet center, M_A is the reconnection Alfvén Mach number, which is the reconnection inflow speed compared to the local Alfvén speed near the current sheet.

As for the total mass m in the flux rope, continuous reconnection brings plasma into the rope through the current sheet successively. So m increases with time. The equation governing such a change reads as(16)

$$\frac{dm}{dt} = B_0 M_A \sqrt{\frac{\rho_0}{\pi}} \frac{\lambda^2 (q - p)(h^2 + \lambda^2)}{(h^2 - y_0^2)(y_0^2 + \lambda^2)} \sqrt{\frac{f(y_0)(q^2 - y_0^2)(y_0^2 - p^2)}{(p^2 + \lambda^2)(q^2 + \lambda^2)}}, \quad (\text{A8})$$

where $f(y)$ is the dimensionless distribution function of the plasma density in the corona, and is related to the mass density distribution $\rho(y)$ in the expression for \tilde{A}_{0h} such that $\rho(y) = \rho_0 f(y)$, ρ_0 being the mass density on the surface of the disk. There is not any existing model of density distribution of a magnetic corona above an accretion disk. If we assume that the physical processes in the accretion-disk corona are similar to that of the Sun, and that the dynamical interface between the differentially rotating disk is analogous to that of the corona-photosphere interface of the sun, we may adopt the solar model, in which $f(y)$ takes the form (e.g., see Lin, Mancuso & Vourlidas 2006 and references therein):

$$f(y) = a_1 z^2(y) e^{a_2 z(y)} [1 + a_3 z(y) + a_4 z^2(y) + a_5 z^3(y)], \quad (\text{A9})$$

where

$$\begin{aligned} z(y) &= \lambda/(\lambda + y), & a_1 &= 0.001272, \\ a_2 &= 4.8039, & a_3 &= 0.29696, \\ a_4 &= -7.1743, & a_5 &= 12.321, \end{aligned}$$

with $f(0) = 1$.

Furthermore, the term F_g in equation (1) is the gravity of the black hole acting on the flux rope, which reads as

$$F_g = \frac{mg_0}{(1 + h/\lambda)^2}, \quad (\text{A10})$$

where g_0 is the gravity near the disk surface in the zeroth order approximation. Substituting equations (A1) through (A10) into equation (1), we are able to solve equation (1) for $\dot{h}(t)$ with initial conditions $h(t=0)$, $\dot{h}(t=0)$, $p(t=0)$, $q(t=0)$, and $m(t=0)$ being given. We assume $h(t=0) = 10 r_g$ where the flux rope starts losing its equilibrium and the eruption commences, $\dot{h}(t=0) = 10^{-5}c$ as an initial perturbation velocity, $p(t=0) = q(t=0) = 0$, and $m(t=0) = m_0$. The results are shown in Figure 2.

Our model have adopted certain approximation to simplify the calculations. We think this is sufficient for illustrating how plasmon ejectas can be expelled from an accretion disk and are accelerated to relativistic field. Note that the gravitational potential is taken to depend only on the flux rope height h although it should be a function of radius $r(\equiv \sqrt{x^2 + y^2})$. This approximation should not affect our result since the gravitational force is not important compared to the magnetic force. Another simplification is that relativistic effects are not included explicitly in equation (1). Special relativity will modify the inertial term, and general relativity will modify the gravity term. While a relativistic version of equation (1) should be used in the future work, even without invoking a full relativistic treatment, we would see from equation (1) that the speed of the plasmon ejecta would approach the speed of light, provided the acceleration region is sufficiently close to the black hole event horizon, as the Lorentz force provided by the flux loop needs to overpower the gravity in order to propel the plasmon ejecta to escape to infinity.

REFERENCES

- Balbus, S. A., Hawley, J. F. *Rev. Mod. Phys.*, 1998, 70, 1
- Blandford, R. D. 2002, in *Lighthouse of the Universe: The Most Luminous Celestial Objects and Their Use for Cosmology*, ed. M. Gilfanov, R. Sunyaev, & Churazov, 38, 1
- Blandford, R. D., Payne, D. G. 1982, *MNRAS*, 199, 883
- Blandford, R. D. & Znajek, R. L. 1977, *MNRAS*, 179, 433
- Corbel, S. et al., 2002, *Science*, 298, 196
- De Villiers, J. P., Hawley, J. F., & Krolik, J. H. 2003, *ApJ*, 599, 1238
- De Villiers, J. P., Hawley, J. F., Krolik, J. H., Hirose, S. 2005, *ApJ*, 620, 878
- Eckart A. et al., 2006, *A&A*, 450, 535
- Fender, R. P. Belloni, T. M. 2004, *ARA&A*, 42, 317

- Fender R. P. et al., 1999, MNRAS, 304, 865
- Fender, R. P. Belloni, T. M. , Gallo, E. 2004, MNRAS, 355, 1105
- Forbes, T. G., Isenberg, P. A. 1991, ApJ, 373, 294
- Hirose, S., Krolik, J. H., De Villiers, J. P., Hawley, J. F. 2004, ApJ, 606, 1083
- Hjellming, R. M., Rupen, M. P. 1995, Nature, 375, 464
- Lin, J. & Forbes, T. G. 2000, J. Geophys. Res., 105, 2375
- Lin, J., Mancuso, S., Vourlidas, A. 2006, ApJ, 649, 1110
- Lin, J., Soon, W., Baliunas, S. L. 2003, New Astron. Rev., 47, 53
- Livio, M., Ogilvie, G. I., Pringle, J. E. 1999, ApJ, 512, 100
- Machida, M. Hayashi, M., Matsumoto, R. 2000, ApJ, 532, L67
- Machida, M., Nakamura, K. Matsumoto, R. 2004, PASJ, 56, 671
- Marscher A. P. et al., 2002, Nature, 417, 625
- Mirabel I. F., et al., 1998, A&A, 330, L9
- Mirabel, I. F., Rodriguez, L. F. 1994, Nature, 371, 46
- Pringle, J. E., Rees, M. J. & Pacholczyk, A. G. 1973, A&A, 29,179
- Shibata, K., Tajima, T., Matsumoto, R. 1990, ApJ, 350, 295
- van der Laan, H. 1966, Nature, 211, 1131
- Yuan, F., Quataert, E., Narayan, R. 2003, ApJ, 598, 301
- Yusef-Zadeh F. et al., 2006, ApJ, 650, 189
- Zhang, M., & Low, B. C. 2005, ARA&A, 43, 103

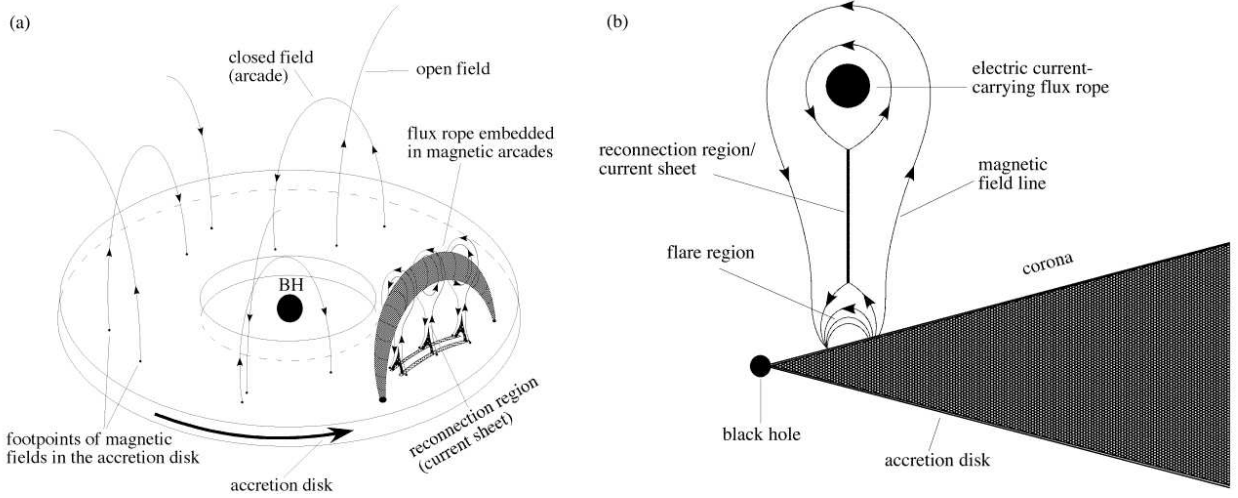


Fig. 1.— Illustration of the formation of a flux rope (panel a) and the ejection of the flux rope and the associated flare (panel b). (a) The accretion flow surrounding the central black hole consists of a main disk body and a corona envelope. Magnetic arcades emerge from the disk into the corona, and a flux rope is formed, as a result of the motion of their footpoints and subsequent magnetic reconnection. Magnetic energy and helicity are continuously transported into the corona and stored in its magnetic field until the energy exceeds a threshold. (b) The flux rope is then ejected, forming a current sheet. Magnetic reconnection occurs in the current sheet, and subsequently the magnetic tension becomes much weaker than the magnetic compression. This results in the energetic ejection of the flux rope. The plasma heated in the magnetic reconnection process produces flares.

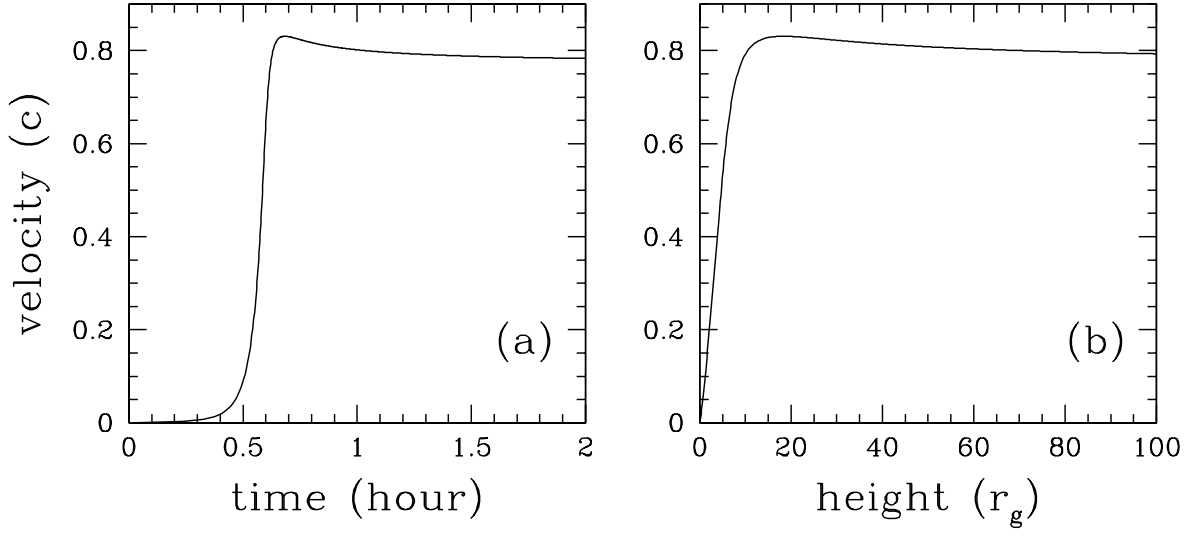


Fig. 2.— The calculated velocity of the ejected plasmon from Sgr A* as a function of time (a) and height (b). The flux rope does not gain the kinetic energy immediately after the catastrophe. Instead it takes about 25 minutes to accelerate from rest to $\sim 0.02c$ because of its inertia and the weakness of the magnetic compression force at the beginning. In the following 10 minutes, the catastrophe together with magnetic reconnection rapidly energize the flux rope and accelerate it to $\sim 0.8c$.